DOI: 10.1002/chem.200501309

Pyrene-Stacked Nanostructures Constructed in the Recombinant Tobacco Mosaic Virus Rod Scaffold

Masayuki Endo,* Hangxiang Wang, Mamoru Fujitsuka, and Tetsuro Majima*[a]

Abstract: The effect of pyrenes introduced into a tobacco mosaic virus (TMV) coat protein monomer on the formation and stability of the TMV assembly was investigated. The possible arrangement of the pyrenes in the inner cavity of the TMV rod was also estimated. The pyrene derivative was introduced to four specific amino acids in the cavity of the TMV rod structure. Rod-structure formation was examined by atomic force microscopy (AFM). Two pyrene-attached mutants (positions 99 and 100) assembled to increase the length of the rod structures by 2.5 μm at pH 5.5. The interaction of the pyrene moieties in the TMV cavity was investigated by steady-state and time-resolved spectroscopic analysis. Strong excimer emission with significantly short wavelength (465 nm) was observed from the two mutants mentioned above. Excitation and UV-visible spectra indicate that the pyrene moieties form π-stacked structures in the TMV cavity. Details of the pyrene interaction were investigated by analyzing the fluorescence lifetime of the excimer. Results suggest that the pyrenes formed preassociated rigid structures with partially overlapped geometry in the restricted space of the TMV cavity. The pyrenes effectively stabilize the TMV rod through a π-stacking interaction in a well-ordered way, and the single pyrene moiety introduced into the monomer affects the overall formation of the TMV rod structure.

Keywords: conjugation · nanostructures · pyrene · self-assembly · tobacco mosaic virus

Introduction

Protein self-assembly is a fundamental issue in biology, as most biological phenomena involve the precise associations of multiple protein units for expression of their functions.[1] Self-assembled protein nanostructures such as tubular, fibrous, and spherical ones are also important for the creation of nanoscale wires and functional materials.[2] The tobacco mosaic virus (TMV) has a hollow cylindrical structure with a high aspect ratio and is formed through the periodical self-assembly of the TMV coat protein (TMVCP) and RNA.[3] Because of its well-characterized nanoscale structure, TMV has been utilized as a template for functionalization with inorganic and organic molecules both in the inner cavity and on the exterior surface.[4–6] Although TMV has such promising features for its application to nanoscale materials, the length of the wild-type TMV rod is limited to 300 nm.[3] For further applications, the rod structure should be extended with suitable modification and functionalization. In the supramolecular assemblies of π-conjugated systems, the π-stacking interactions between molecular units contributes to the formation and stabilization of the supramolecular structures.[7] In the π-systems that function in water, the double-helix DNA structure is stabilized by base pairing and π-stacking of the heterocyclic bases, and some peptides are also stabilized by the π-stacking of aromatic molecules.[8] Therefore, the promotion of the TMV supramolecular assembly and subsequent extension of the TMV rod structure can be achieved by selective incorporation of aromatic molecules into the TMVCP monomers based on the TMV crystal structure.[9] In addition, the novel π conjugated system can also be constructed in the TMV rod structure by self-assembly of the designed TMVCP–aromatic-molecule conjugates for the creation of functional nanomaterials.

In this report, we investigated the effect of aromatic molecules on the formation and stability of TMV rod structures. Pyrene was introduced into specific positions in the inner cavity of the TMV rod. We examined the rod-structure formation by performing atomic force microscopy (AFM). The

[a] Dr. M. Endo, H. Wang, Dr. M. Fujitsuka, Prof. Dr. T. Majima
The Institute of Scientific and Industrial Research, Osaka University
8–1 Mihogaoka, Ibaraki, Osaka 567–0047 (Japan)
Fax: (+81) 6-6879-8499
E-mail: endo@sanken.osaka-u.ac.jp
majima@sanken.osaka-u.ac.jp

Supporting information for this article is available on the WWW under http://www.chemeurj.org/ or from the author.

interaction and behavior of the pyrene moieties in the cavity of the TMV rod were investigated by steady-state and time-resolved spectroscopic analysis of the characteristic fluorescence of the pyrene monomers and excimers. We also estimated the possible arrangement of the pyrenes in the TMV cavity using these spectral data.

Results and Discussion

Preparation of pyrene-attached TMVCP monomers: The pyrene derivative was incorporated into specific amino acids located on the flexible loop of the TMVCP monomer near the interior surface of the TMV assembly (Figure 1). For incorporation of pyrene into the cavity of the rod structure, we selected four amino acids on the flexible loop, N98, Q99, A100, and N101, and individually mutated them to a cysteine residue. A pyrene was then selectively introduced to the cysteine residue by using *N*-(1-pyrene)maleimide. The edge-to-edge length of a pyrene maleimide molecule is 1.2 nm, which is small enough to be incorporated into the inner cavity with diameter of 4 nm. Because the wild-type TMVCP has one cysteine residue at position 27, the Cys27 was first replaced by alanine, and four amino acids on the inner loop were then individually changed to cysteine for the selective labeling with pyrene maleimide.

Expression and purification of the recombinant TMVCP and mutants were carried out according to the previously reported method with some modification (see Supporting Information).[10] Selective introduction of the pyrene moiety into the TMVCP cysteine mutants was carried out by treatment with pyrene maleimide in a solution of pH 8.0 to minimize monomer aggregation. Identification of the products and the efficiencies of pyrene incorporation into the cysteine mutants were examined by MALDI-TOF mass spectrometry. A major peak corresponding to the molecular weight of the pyrene-attached TMVCP and a minor one originating from the unlabeled cysteine mutant were observed (Figure S2). Based on the mass spectrometry data, the efficiencies of pyrene incorporation into the cysteine mutants were estimated to be around 90%.

Pyrene-attached TMV nanostructures: The formation of the TMV rod structure under conditions of pH 5.5 and 7.6 was investigated by AFM. The samples (pH 8) for both the cysteine- and pyrene-modified mutants were dialyzed at pH 5.5 for rod-structure formation, and then the samples at pH 7.6 were prepared by increasing the pH value from 5.5 to 7.6. As the cysteine mutants assembled at pH 5.5, rod structures with heights of 15–18 nm and lengths of approximately 300 nm were observed for all the cysteine mutants (Figure S3). This indicates that the modification at C27A and the cysteines introduced to the four positions do not affect the formation of the TMV rod structures. Under the pH 7.6 conditions, the rod structures disassembled into disk structures.[3] These results clearly show that the cysteine mutants maintain their intrinsic properties of self-assembly and disassembly in a pH-dependent manner.

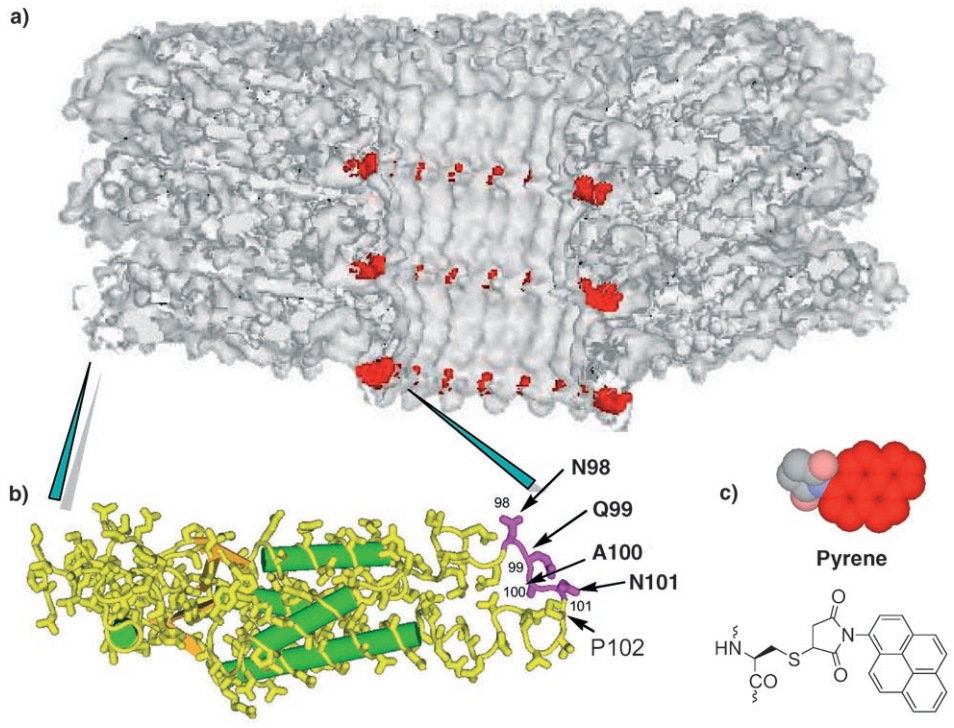

Figure 1. a) Crystal structure of the TMV assembly. Sectional view of the TMV supramolecular structure and the inner cavity (4 nm diameter). Amino acid Q99 on the surface of the cavity is represented in red. b) TMVCP monomer and four amino acids (N98, Q99, A100, and N101) on the loop, which were selectively mutated to cysteine for introduction of a pyrene moiety. c) Pyrene was introduced to the selectively mutated cysteine residues by maleimide–thiol coupling using *N*-(1-pyrene)maleimide.

The rod-structure formation of the four pyrene-attached TMVCP mutants was also analyzed by AFM. The AFM images are shown in Figure 2, and the distribution of the TMV rods is summarized in Figure 3. The C27A/N98C-pyrene and C27A/N101C-pyrene mutants showed a similar tendency for rod-structure formation. In these pyrene-attached mutants, rod structures with a slightly extended length (maximum 600–800 nm), relative to those of the unmodified TMVCP, were observed at pH 5.5 (Figure 2a and d, respectively), and the rod structures were completely disassembled

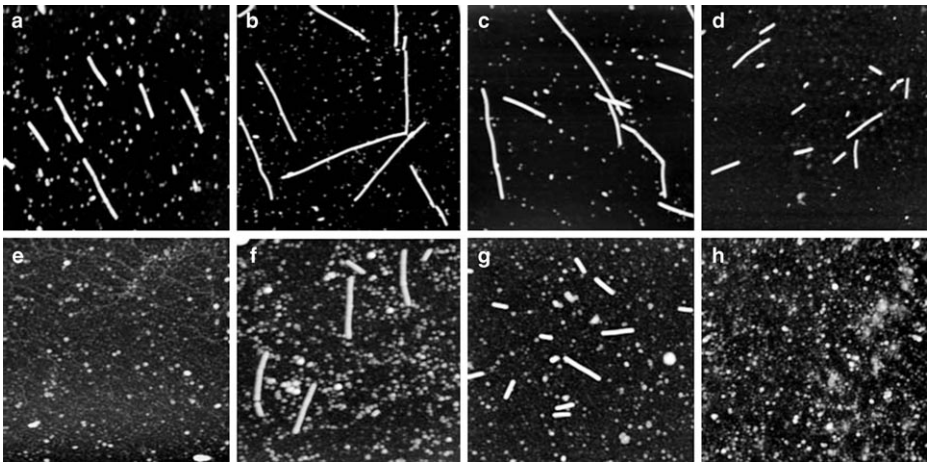

Figure 2. AFM images of pyrene-modified TMV rod structures at lower and higher pH. a) and e): C27A/N98C-pyrene mutant at pH 5.5 and 7.6, respectively. b) and f): C27A/Q99C-pyrene mutant at pH 5.5 and 7.6, respectively. c) and g): C27A/A100C-pyrene mutant at pH 5.5 and 7.6, respectively. d) and h): C27A/N101C-pyrene mutant at pH 5.5 and 7.6, respectively. The size of each image is 3×3 μm.

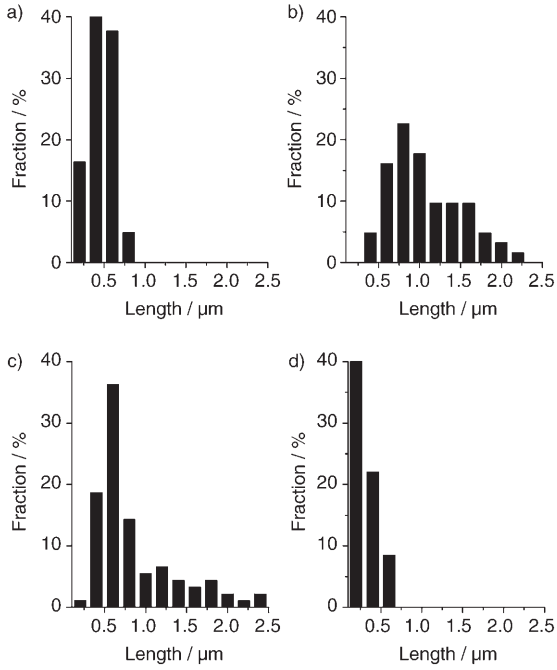

Figure 3. Distribution of the length of the pyrene-attached TMV rods at pH 5.5: a) C27A/N98C-pyrene mutant, b) C27A/Q99C-pyrene mutant, c) C27A/A100C-pyrene mutant, d) C27A/N101C-pyrene mutant.

at pH 7.6 (Figure 2e and h, respectively). In contrast, in the cases of the C27A/Q99C-pyrene and C27A/A100C-pyrene mutants, rod structures with significantly extended lengths (maximum length 1.85 and 2.45 μm, respectively), 6–8 times longer than the native TMV rod, were formed at pH 5.5 (Figure 2b and c, respectively). These results indicate that the incorporation of a pyrene moiety at positions 99 and 100 significantly promotes the assembly of TMVCP. In addition, these two pyrene-modified TMV still maintained the rodlike structures at pH 7.6 (Figure 2f and g), which also indicates that the incorporation of pyrene moieties at these positions stabilizes rod structures under higher pH conditions. These results suggest that the pyrene modification promotes rod-structure formation, and the extension of the rod structures with pyrene is strongly dependent on the positions at which the pyrene moiety is introduced.

Photochemical properties of the pyrenes in the TMV rod structure: To examine the interaction of the pyrene moieties in the rod structure, we utilized the fluorescence properties of pyrene. Pyrene is a well-known photophysical probe for detecting molecular interactions by monitoring emission of the pyrene excimer.[11–13] The characteristic excimer fluorescence also provides information concerning the distance and geometry between neighboring pyrene moieties.[11–13] In the rod structure of the TMV, the positions 98, 99, 100, and 101 are located on the flexible loop in the inner cavity. As the rod structures are formed, the neighboring pyrene moieties can become accessible to each other to form pyrene dimer structures. The fluorescence spectra for four pyrene-attached mutants were obtained at pH 5.5 (Figure 4). By using 345 nm light for excitation, emission bands (377–395 nm) assigned to the pyrene monomer in the singlet excited state were observed. In addition, a broad emission band at around 465 nm assigned to pyrene excimer emission was observed for all the mutants. The C27A/Q99C-pyrene and C27A/A100C-pyrene mutants showed very strong excimer emissions relative to those of the C27A/N98C-pyrene and C27A/N101C-pyrene mutants. This indicates that the pyrene

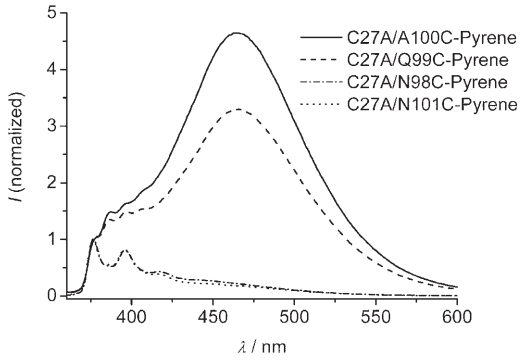

Figure 4. Fluorescence spectra of pyrene-attached TMVCP mutants at pH 5.5. Excitation wavelength: $\lambda_{ex} = 345$ nm. All spectra were normalized to the (0,0) peak at 377 nm.

moieties in the C27A/Q99C-pyrene and C27A/A100C-pyrene mutants are located close enough to form pyrene dimers and excimers. The intensity of excimer emission of the C27A/A100C-pyrene mutant was higher than that of the C27A/Q99C-pyrene mutant, which means that the formation of pyrene dimer and excimer also depends on the position of modification on the inner loop of the TMVCP monomer. The pyrene moieties of the C27A/A100C-pyrene mutant occupy the most suitable positions in the inner cavity of the TMV rod for the formation of dimers and excimers. Interestingly, the efficiency of excimer formation is consistent with the length of the TMV rods of the pyrene-attached TMVCP mutants (see AFM images in Figure 2). These results indicate that the interactions between pyrenes contribute to the elongation of the TMV rod structures. The notably short wavelength of excimer emission (465 nm) is also a unique character of the pyrene excimer in the TMV cavity.

In addition, the excitation spectra for the emission of the monomer ($\lambda_{em}=375$ nm) and excimer ($\lambda_{em}=465$ nm) of the C27A/Q99C-pyrene and C27A/A100C-pyrene mutants were recorded (Figure S4). Under the same conditions of pH 5.5, the peak-to-valley ratios (P_M) for the (0,0) transition bands for the monomers of the C27A/Q99C-pyrene and C27A/A100C-pyrene mutants were 1.57 and 1.45, respectively. In the excitation spectra for the excimers of these mutants, the peak-to-valley ratios (P_E) for the (0,0) transition bands were 1.26 and 1.25, respectively. The 2 nm shift for the (0,0) transition bands was observed for the pyrene-attached mutants of both the excimers (345 nm) and monomers (343 nm). The $P_E < P_M$ and the red-shift of the (0,0) transition band of the excimer from that of the monomer are usually observed for the preassociated pyrene structures.[12] The results observed indicate the possible preassociation of the pyrene moieties in the cavity of the TMV rod structures.

To investigate the pyrene association further, we recorded the UV-visible spectrum of the C27A/A100C-pyrene mutant at pH 5.5 (Figure S5). The peak-to-valley ratio (P_A) observed for the (0,0) transition bands (345 nm, $P_A=1.18$) decreased relative to that of the C27A/N98C-pyrene mutant (344 nm, $P_A=1.30$), which formed excimer only slightly. This corresponds to the broadening of the absorption bands of the C27A/A100C-pyrene mutant and means that pyrenes in the C27A/A100C-pyrene mutant have a stronger π-interaction than those in the C27A/Q98C-pyrene mutant.[11]

pH-dependence of pyrene excimer formation: To examine the dependence of excimer emission on the pH values of the solutions, we measured the fluorescence spectra at pH 5.5, 6.5, and 7.5 (Figure 5). For the C27A/Q99C-pyrene mutant, the excimer emission gradually decreased as the pH value increased. In addition, the excimer peak shifted to a longer wavelength (from 465 to 468 nm) as the pH was changed from 6.5 to 7.5. Most of the TMV rods disassembled into the disk structure at pH 7.6, as shown in the AFM images in Figure 2. The wavelength of the excimer peak reflects the overlapping geometry of two pyrene moieties,[12,13] thus, this red-shift would be attributed to the rearrangement

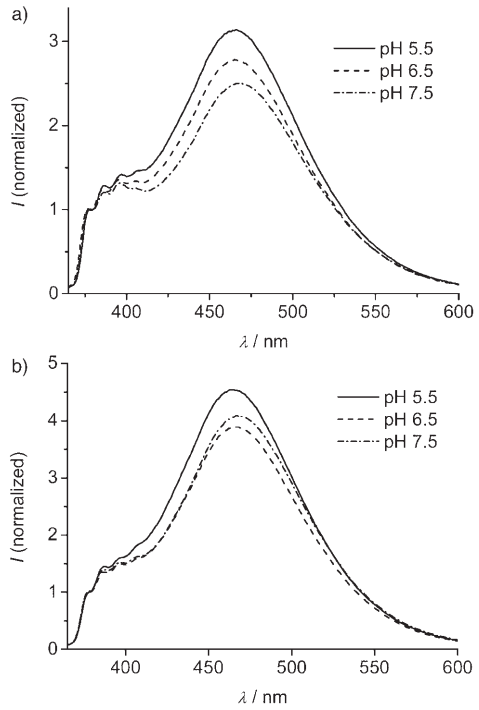

Figure 5. pH-dependence of the fluorescence spectra of the pyrene-modified TMVCP mutants: a) C27A/Q99C-pyrene mutant and b) C27A/A100C-pyrene mutant. Excitation wavelength: $\lambda_{ex}=345$ nm. All spectra were normalized to the (0,0) peak at 377 nm.

of the pyrene moieties from a rigid-packed to a more relaxed conformation in the TMV cavity. The C27A/A100C-pyrene mutant also showed a decrease in excimer emission as the pH increased from 5.5 to 6.5. The excimer peak also showed a red-shift (465 to 469 nm) with a slight increase in emission as the pH value increased from 5.5 to 7.5.

We also examined the formation of the rod structure with pyrene-labeled TMVCP by mixing the pyrene-labeled TMVCP and unlabeled TMVCP in a 1:1 ratio. The TMVCP monomers were mixed at pH 8.0, then the pH was lowered to 5.5 by dialysis. For the pyrene-labeled mutants at positions 99 and 100, the pyrene excimer of the mixture significantly decreased relative to those of the pyrene-labeled TMVCP (Figure S6). The excimer formation in the cavity of the TMV rod is easily disrupted by the addition of the non-labeled monomers, because pyrenes were separated by the non-labeled monomers. The results indicate that the formation of the rod structure is directed mainly by interaction of the TMVCP monomer, and the pyrenes simply assist the extension of the rod structures.

Behavior of the pyrenes in the inner cavity of the TMV rod structure: To characterize the details of the association of the pyrene moieties in the TMV cavity, we measured the fluorescence lifetimes of emissions of both the pyrene monomer and excimer under the various pH conditions. In the case of the C27A/Q99C-pyrene and C27A/A100C-pyrene mutants at pH 5.5, the rise of the excimer emission was not observed on the timescale of a few ns, indicating

Table 1. Fluorescence lifetimes (τ_1 and τ_2) of the pyrene monomer and excimer of the C27A/Q99C-pyrene and C27A/A100C-pyrene mutants under various pH conditions.[a]

		Monomer				Excimer			
TMVCP mutant	pH	τ_1[ns]	τ_2[ns]	f_1	f_2	τ_1[ns]	τ_2[ns]	f_1	f_2
C27A/Q99C-pyrene	5.5	8.6	52.9	0.81	0.19	5.7	41.7	0.65	0.35
	6.5	8.2	59.8	0.81	0.19	6.1	43.8	0.70	0.30
	7.5	7.0	61.8	0.79	0.21	6.7	46.8	0.70	0.30
C27A/A100C-pyrene	5.5	7.5	56.4	0.86	0.14	5.7	39.6	0.72	0.28
	6.5	7.9	53.9	0.80	0.20	6.5	43.4	0.65	0.35
	7.5	7.4	53.4	0.86	0.14	6.5	45.1	0.60	0.40

[a] Measurement conditions are described in the Experimental Section. The f_1 and f_2 values denote the fractions of the lifetimes of τ_1 and τ_2, respectively.

that the pyrenes in the cavity of the rod structures exist in a static form at pH 5.5, which is different from the pyrenes attached to the polymer scaffolds.[14,15]

The relationship between the fluorescence lifetimes and pH values is summarized in Table 1. The lifetimes of both the monomers and excimers were fitted to two exponential terms; one had a shorter lifetime and the other had the normal lifetime of pyrene fluorescence, which were similar to the pyrene-attached polymers.[15] The short lifetime of the pyrene monomers (7.0–8.6 ns) may be attributed to the rapid formation of the pyrene excimers, although the rise of the pyrene excimer, which indicates the dynamic excimer formation, was not observed. An explanation for this could be that the formation of the pyrene excimers is obscured by the very rapid quenching that occurs on the time scale of 2–3 ns. In the case of the excimer, because the multiple pyrenes are densely packed in the inner cavity of the TMV rod, the rapid quenching of the pyrene excimer by the neighboring pyrene moieties would occur within the short excimer lifetimes (5.7–6.7 ns).

For both pyrene-attached mutants, the longer lifetimes of the pyrene excimer gradually increased as the pH values increased from 5.5 to 7.5. This indicates that the pyrene excimers in the cavity of the TMV rod gradually change conformation in response to pH. At pH 5.5, the TMVCP forms the rod structures as observed in the AFM images (Figure 2). Normally, the rod structures of the unmodified TMVCP disassemble into the disk structures at neutral pH.[3] These results indicate that the pyrene moieties in the disk structures can maintain their interaction with a conformation slightly different to that of the pyrene moieties in the rod structures. Because the difference in the excimer lifetimes between the rod and disk structures is small, it was difficult to distinguish the disk structures from the rod structures at pH 7.5 by analysis of the fluorescence lifetimes of the pyrene excimers in this study.

Finally, we estimated the locations of the pyrenes in the cavity by analyzing the crystal structure of TMV and the results of excimer formation. The distances between the α-carbons of the neighboring monomers in the TMV rod structure were 1.03 nm for N98 residues, 1.04 nm for Q99 residues, 1.04 nm for A100 residues, and 0.95 nm for N101 residues. The distances between the α-carbons in the crystal are, therefore, similar at around 1.0 nm.[9] The pyrene at position 98 is buried inside the interior surface, and two neighboring pyrenes were too far away to make contact. In contrast, the positioning of pyrenes at positions 99 and 100 on the surface of the cavity can facilitate excimer formation, due to their location and orientation being favourable for interaction. In the case of the pyrene at position 101, because the adjacent proline 102 restricts the rotation of the peptide chain, the consequently unfavorable orientation of the side chain of position 101 may limit pyrene interaction to form excimers. In addition, the arrangement of the pyrene moieties in the TMV cavity was estimated. Because of the significantly short emission wavelength (465 nm) and lifetime (ca. 40 ns) of the excimer compared to those of the bis-pyrenyl compounds, neighboring pyrene moieties have a partially overlapped geometry as a rigid form in the cavity.[13] Therefore, the molecular planes of the multiple pyrene rings may be arranged into a restricted conformation, leading to a π-stacked helical structure for the self-assembly of the TMVCP monomers, without inhibiting the formation of the TMV rod structure.

Conclusion

We have demonstrated the effect of the pyrene moiety on the formation of rod structures and have characterized the photochemical properties and arrangement of the pyrene moieties in the cavity of the TMV rod. The pyrenes were packed into the inner cavity of the TMV rod without affecting the intrinsic properties of TMV assembly, and the length of the rod structures was extended by the π-stacking interaction of the pyrene moieties. Multiple pyrenes formed preassociated structures with a partially overlapped geometry in the TMV cavity. The TMV supramolecular system described allows the integration of aromatic molecules into the cavity of the TMV scaffold and serves to create well-ordered, self-assembled molecular wires.[7] Furthermore, despite the pyrene-attached TMV nanostructures, the diameter of the cavity inside was maintained at 2.5 nm, which may allow for the incorporation of functional molecules and polymers for the construction of functional nanomaterials.

Experimental Section

Introduction of pyrene maleimide to TMVCP cysteine mutants: The four cysteine mutants were labeled with *N*-(1-pyrene)maleimide according to a previously reported method.[16] For introduction of pyrene to the cysteine mutant, the mutant (100 μg mL^{-1}) was treated with dithiothreitol (DTT, 2-fold excess) for 2 h at 37 °C to completely reduce the cysteine residue, and then reacted with *N*-(1-pyrene)maleimide (dimethyl sulfoxide (DMSO) solution, 10-fold excess) in a 20 mM Tris-HCl (pH 8.0) solu-

tion at 37 °C for 2 h. The unreacted pyrene was removed by a gel filtration column (Sephadex G-25; Pharmacia) pre-equilibrated with the same buffer (pH 8.0). The pyrene-modified mutants were analyzed by MALDI-TOF mass spectroscopy (Figure S2); MALDI-TOF MS (positive): *m*/*z* calcd for C27A/N98C-pyrene: 17867.1; found: 17845.6; *m*/*z* calcd for C27A/Q99C-pyrene: 17853.0; found: 17854.4; *m*/*z* calcd for C27A/A100C-pyrene: 17910.1; found: 17885.8; *m*/*z* calcd for C27A/N101C-pyrene: 17867.1; found: 17859.4. For the rod-structure formation at pH 5.5, the pyrene-attached TMVCP samples (1 mL) were dialyzed against 2 L of a buffer containing 20 mM phosphate buffer (pH 5.5) at 4 °C overnight.

Atomic force microscopy: AFM images were acquired by using atomic force microscopy (SPA400-DFM, Seiko Instruments) in the dynamic-force mode. The sample containing the TMVCP monomer (50 $\mu g\,mL^{-1}$) in 20 mM sodium phosphate buffer (5 μL) was placed on a freshly cleaved mica plate pretreated with 0.01 % aminopropyltriethoxysilane, adsorbed for 5 min at RT, and then dried by gentle air blowing.

Steady-state spectroscopic measurements: The fluorescence and UV/Vis spectra were acquired by using a Hitachi 850 spectrofluorometer and JASCO V-530 spectrophotometer, respectively. The samples (1 mL) were prepared by using dialyzed pyrene-attached TMVCPs (80 $\mu g\,mL^{-1}$, 4.5 μM) in 20 mM sodium phosphate buffer (pH 5.5). The measurements were performed at 23 °C in a 1-cm path-length quartz cell. For the pH-dependent experiments, the pH was stepwise increased from 5.5 to 7.5 by addition of a NaOH solution and directly monitoring the pH with a pH meter.

Fluorescence lifetime measurements: Fluorescence decays were acquired by the single-photon-counting method using a streak scope (Hamamatsu Photonics, C4334–01) equipped with a polychromator (Acton Research, SpectraPro150). The ultrashort laser pulse was generated by a Ti:sapphire laser (Spectra-Physics, Tsunami 3941-M1BB, fwhm 100 fs) pumped with a diode-pumped solid-state laser (Spectra-Physics, Millnnia VIIIs). For excitation of the sample, the output of the Ti:sapphire laser was converted to THG (310 nm) with a harmonic generator (Spectra-Physics, GWU-23FL). Measurements were made at 23 °C in a solution containing 4.5 μM TMVCP-pyrene under various pH conditions. Data in the wavelength ranges of 375–390 nm and 460–500 nm were collected for calculation of the monomer and excimer lifetimes, respectively.

Acknowledgements

This work was supported partly by a Grant-in-Aid for Scientific Research on Priority Area (417), 21st Century COE Research, and a grant from the Ministry of Education, Culture, Sports, Science, and Technology (MEXT) of the Japanese Government.

[1] *Introduction to Protein Structures* (Eds.: C. Branden, J. Tooze), Garland Publishing, New York, **1999**.
[2] a) C. M. Niemeyer, *Angew. Chem.* **2001**, *113*, 4254–4287; *Angew. Chem. Int. Ed.* **2001**, *40*, 4128–4158; b) E. Katz, I. Willner, *Angew. Chem.* **2004**, *116*, 6166–6235; *Angew. Chem. Int. Ed.* **2004**, *43*, 6042–6108.
[3] A. Klug, *Angew. Chem.* **1983**, *95*, 579–596; *Angew. Chem. Int. Ed. Engl.* **1983**, *22*, 565–582.
[4] T. Shimizu, M. Masuda, H. Minamikawa, *Chem. Rev.* **2005**, *105*, 1401–1443.
[5] a) W. Shenton, T. Douglas, M. Young, G. Stubbs, S. Mann, *Adv. Mater.* **1999**, *11*, 253–256; b) E. Dujardin, C. Peet, G. Stubbs, J. N. Culver, S. Mann, *Nano Lett.* **2003**, *3*, 413–417; c) M. Knez, A. M. Bittner, F. Boes, C. Wege, H. Jeske, E. Maiss, K. Kern, *Nano Lett.* **2003**, *3*, 1079–1082; d) M. Knez, M. Sumser, A. M. Bittner, C. Wege, H. Jeske, P. Martin, K. Kern, *Adv. Funct. Mater.* **2004**, *14*, 116–124.
[6] T. L. Schlick, Z. Ding, E. W. Kovacs, M. B. Francis, *J. Am. Chem. Soc.* **2005**, *127*, 3718–3723.
[7] a) F. J. Hoeben, P. Jonkheijm, E. W. Meijer, A. P. H. J. Schenning, *Chem. Rev.* **2005**, *105*, 1491–1546; b) A. P. H. J. Schenning, E. W. Meijer, *Chem. Commun.* **2005**, 3245–3258.
[8] a) E. Gazit, *FASEB J.* **2002**, *16*, 77–83; b) J. Liu, W. Yong, Y. Deng, N. R. Kallenbach, M. Lu, *Proc. Natl. Acad. Sci. USA* **2004**, *101*, 16156–16161; c) V. Kayser, D. A. Turton, A. Aggeli, A. Beevers, G. D. Reid, G. S. Beddard, *J. Am. Chem. Soc.* **2004**, *126*, 336–343.
[9] a) R. Pattanayek, G. Stubbs, *J. Mol. Biol.* **1992**, *228*, 516–528; b) B. Bhyravbhatla, S. J. Watowich, D. L. D. Caspar, *Biophys. J.* **1998**, *74*, 604–615.
[10] a) D. Hwang, I. M. Roberts, T. M. A. Wilson, *Proc. Natl. Acad. Sci. USA* **1994**, *91*, 9067–9071; b) S. J. Shire, P. McKay, D. W. Leung, G. J. Cachianes, E. Jackson, W. I. Wood, *Biochemistry* **1990**, *29*, 5119–5126.
[11] *Molecular Fluorescence: Principles and Applications* (Ed.: B. Valeur), Wiley-VCH, **2002**.
[12] F. M. Winnik, *Chem. Rev.* **1993**, *93*, 587–614.
[13] F. C. De Schryver, P. Collart, J. Vandendriessche, R. Goedeweeck, A. Swinnen, M. van der Auweraer, *Acc. Chem. Res.* **1987**, *20*, 159–166.
[14] a) H. Ringsdorf, J. Venzmer, F. M. Winnik, *Macromolecules* **1991**, *24*, 1678–1686; b) M. A. Winnik, S. M. Bystryak, Z. Liu, J. Siddiqui, *Macromolecules* **1998**, *31*, 6855–6864.
[15] a) J. Matsui, M. Mitsuishi, T. Miyashita, *J. Phys. Chem. B* **2002**, *106*, 2468–2473; b) J. Duhamel, S. Kanagalingam, T. J. O'Brien, M. W. Ingtatta, *J. Am. Chem. Soc.* **2003**, *125*, 12810–12822.
[16] D. Sahoo, V. Narayanaswami, C. M. Kay, R. O. Ryan, *Biochemistry* **2000**, *39*, 6594–6601.

Received: October 21, 2005
Published online: February 28, 2006

